

# Review of Serial and Parallel Min-Cut/Max-Flow Algorithms for Computer Vision

Patrick M. Jensen, Niels Jeppesen, Anders B. Dahl, and Vedrana A. Dahl

**Abstract**—Minimum cut / maximum flow (min-cut/max-flow) algorithms are used to solve a variety of problems in computer vision and thus significant effort has been put into developing fast min-cut/max-flow algorithms. This makes it difficult to choose an optimal algorithm for a given problem – especially for parallel algorithms, which have not been thoroughly compared. In this paper, we review the state-of-the-art min-cut/max-flow algorithms for unstructured graphs in computer vision. We evaluate run time performance and memory use of various implementations of both serial and parallel algorithms on a set of graph cut problems. Our results show that the Hochbaum pseudoflow algorithm is the fastest serial algorithm closely followed by the Excesses Incremental Breadth First Search algorithm, while the Boykov-Kolmogorov algorithm is the most memory efficient. The best parallel algorithm is the adaptive bottom-up merging approach by Liu and Sun. Additionally, we show significant variations in performance between different implementations the same algorithms highlighting the importance of low-level implementation details. Finally, we note that existing parallel min-cut/max-flow algorithms can significantly outperform serial algorithms on large problems but suffers from added overhead on small to medium problems. Implementations of all algorithms are available at: [github.com/patmjensen/maxflow\\_algorithms](https://github.com/patmjensen/maxflow_algorithms).

**Index Terms**—Algorithms, computer vision, graph algorithms, graphs-theoretic methods, parallel algorithms, performance evaluation of algorithms and systems

## 1 INTRODUCTION

MIN-CUT/MAX-FLOW algorithms are ubiquitous in computer vision since a large variety of computer vision problems can be formulated as min-cut/max-flow problems. Example applications include image segmentation [9, 12, 33, 34, 39, 55], stereo matching [10, 44], surface reconstruction [47], surface fitting [16, 40, 46, 48, 64, 67], and texture restoration [58]. In recent years, min-cut/max-flow algorithms have also found use in conjunction with deep learning methods – for example, to quickly generate training labels [41] or in combination with convolutional neural networks (CNNs) [28, 53, 61].

Formally, min-cut/max-flow algorithms in computer vision are used for solving energy minimization problems with an energy function,  $\mathcal{E}$ , of the form

$$\mathcal{E}(\mathbf{x}) = \sum_{i \in V} \mathcal{E}_i(x_i) + \sum_{(i,j) \in V \times V} \mathcal{E}_{ij}(x_i, x_j), \quad (1)$$

where  $V$  is a set of binary variables  $x_i$ ,  $\mathcal{E}_i$  is a unary term associated with variable  $x_i$  and  $\mathcal{E}_{ij}$  is a binary term associated with the pair of variables  $x_i, x_j$ . In a typical application, such as binary segmentation with Markov random fields (MRFs) [9],  $V$  represents pixels in an image and  $x_i$  represents the assignment of pixel  $i$ . However, variables can also describe more abstract things such as candidate positions for mesh vertices [16, 48, 64, 66].

For energy functions which are *submodular*, meaning that all binary energy terms satisfy the condition

$$\mathcal{E}_{ij}(0, 0) + \mathcal{E}_{ij}(1, 1) \leq \mathcal{E}_{ij}(0, 1) + \mathcal{E}_{ij}(1, 0), \quad (2)$$

the minimization can be solved directly as a min-cut/max-flow problem [19, 45]. If the energy function is not submodular, one can

either use a submodular approximation or an approach based on quadratic pseudo-Boolean optimization (QPBO) as described in [7, 29, 43, 58].

Due to the wide applicability of min-cut/max-flow in computer vision, several fast generic min-cut/max-flow algorithms have been developed [9, 25, 30]. Based on these generic algorithms, more specialized algorithms have been created that exploit the grid structure of images to reduce memory use and run time [35, 36, 57, 63]. Furthermore, methods for dynamic problems [25, 42, 68], where a series of similar min-cut/max-flow problems are solved in succession, have been examined. For such problems, the results of the first solution can be reused to find the subsequent solutions much faster than the first. Finally, some papers [15, 59, 60, 68, 69] have explored methods to solve min-cut/max-flow problems in a distributed fashion, where the computations may be split across several computational nodes. This approach is primarily suited for graphs that are too large to fit in physical memory.

In this paper, we focus on generic min-cut/max-flow algorithms, which do *not* make assumptions about the graph structure (e.g., requiring a grid structure). Furthermore, we consider static problems, where a solution is calculated once, without access to a previous solution (as opposed to dynamic problems). Finally, we do not consider whether the algorithm works well in a distributed setting, but focus only on the case where the complete graph can be loaded into physical memory.

The goal is that our experimental results can help researchers understand the strengths and weaknesses of the current state-of-the-art min-cut/max-flow algorithms and help practitioners when choosing a min-cut/max-flow algorithm to use for a given problem.

### 1.1 Related Work

In this section, we give an overview of existing papers which have surveyed and/or compared serial and parallel min-cut/max-flow algorithms.

• P. M. Jensen, N. Jeppesen, A. B. Dahl, and V. A. Dahl are with the Department of Applied Mathematics and Computer Science, Technical University of Denmark, Kongens Lyngby, Denmark.  
E-mail: {patmjensen, niejep, abda, vand}@dtu.dk

### 1.1.1 Serial Algorithms

Several papers [11, 17, 25, 62] provide comparisons of different serial min-cut/max-flow algorithms on a variety of standard benchmark problems. However, many of these benchmark problems no longer reflect the scale and/or structure of modern vision problems solved using min-cut/max-flow, as they consist of small problems and/or grid graphs. Furthermore, [11, 17, 62] do not include all current state-of-the-art algorithms, while other papers do not include initialization times for the min-cut computation. As shown by Verma and Batra [62], it is important for practical use to include the initialization time, as algorithms (or, specifically, their implementations) may spend as much time on initialization as on the min-cut computation. Finally, existing papers only compare reference implementations<sup>1</sup> of the different algorithms — the exception being that an optimized version of the BK algorithm is sometimes included, e.g. in [25]. However, as implementation details can significantly impact performance [62], it is difficult to separate the practical performance of the algorithm from that of the implementation. As a result, based on the existing literature, it is difficult to assess how much of the performance improvements in more recent algorithms are due to better algorithmic choices versus low-level implementation optimizations.

### 1.1.2 Parallel Algorithms

To our knowledge, a systematic comparison between parallel min-cut/max-flow algorithms has not been made. Papers introducing parallel algorithms only compare with serial algorithms [49, 60, 69] or a single parallel algorithm [6]. The most comprehensive comparison so far was made by Shekhovtsov and Hlaváč [59] who included a generic and grid-based parallel algorithm. However, due to the lack of a publicly available implementation, no paper compares with the approach by Liu and Sun [49], even though it is expected to be the fastest [59, 60]. In addition, all papers use the same set of computer vision problems used to benchmark the serial algorithms. This is not ideal, as the set lacks larger problems and we expect large problems to benefit the most from parallelization. As a result, the performance benefit of parallel algorithms may be underestimated and we lack information about the performance of the parallel algorithms for large problems. In other words, we are likely lacking information about the performance of the parallel algorithms for the size of problems, where parallel algorithms are the most relevant.

## 1.2 Contributions

We evaluate current state-of-the-art generic serial and parallel min-cut/max-flow algorithms on a number of computer vision problems with varying graph structures. We compare the algorithms on commonly used benchmark problems, as well as several new problems, which better reflect the scale of modern vision problems — especially in the realm of 3D image segmentation.

For the serial algorithms, we evaluate the reference implementations of the Hochbaum pseudoflow (HPF) algorithm [30, 31] and the preflow push-relabel (PPR) [24] algorithms. Furthermore, to reduce the influence of the implementation details, we evaluate different versions (including our own) of both the Excesses Incremental Breadth First Search (EIBFS) [25] algorithm and the Boykov-Kolmogorov (BK) [9] algorithm. We chose these for

an extended evaluation as EIBFS is the most recent min-cut/max-flow algorithm and BK is still widely used in the computer vision community.

For the parallel algorithms, we provide the first comprehensive comparison of all major approaches. This includes our own implementation of the bottom-up merging algorithm by Liu and Sun [49], our own version of the reference implementation of the dual decomposition algorithm by Strandmark and Kahl [60], the reference implementation of the dual region discharge algorithm by Shekhovtsov and Hlaváč [59], and an implementation of the parallel preflow push-relabel algorithm by Baunstark et al. [6]. In our comparison, we evaluate not just the run time — including both the initialization time and the time for the min-cut/max-flow computations — but also the memory use of the algorithms. Memory usage has not received much attention in the literature, despite it often being a limiting factor when working with large problems. All of our implementations are available at (link to come).

## 2 SERIAL MIN-CUT/MAX-FLOW ALGORITHMS

Serial min-cut/max-flow algorithms can be divided into three families: augmenting paths, preflow push-relabel, and pseudoflow algorithms. In this section, we provide an overview of how algorithms from each family work. However, we will first introduce our notation and define the min-cut/max-flow problem.

We define a directed graph  $G = (V, E)$  by its set of *nodes*,  $V$ , and its set of directed *arcs*,  $E$ . We let  $n$  and  $m$  refer to the number of nodes and arcs, respectively. Each arc  $(i, j) \in E$  is assigned a non-negative *capacity*  $c_{ij}$ . For min-cut/max-flow problems, we define two special *terminal nodes*,  $s$  and  $t$ , which are referred to as the *source* and *sink*, respectively. Arcs to and from these nodes are known as *terminal arcs*.

A *feasible flow* in the graph  $G$  is an assignment of non-negative numbers (flows),  $f_{ij}$ , to each arc  $(i, j) \in E$ . A feasible flow must satisfy the following two constraints: *capacity constraints*,  $f_{ij} \leq c_{ij}$ , and *conservation constraints*,  $\sum_{(i,j) \in E} f_{ij} = \sum_{(j,k) \in E} f_{jk}$  for all nodes  $j \in V \setminus \{s, t\}$ . Capacity constraints ensure that the flow along an arc does not exceed its capacity. Conservation constraints ensure that the flow going into a node equals the flow coming out. A given feasible flow also induces a *residual graph* where the set of *residual arcs*,  $R$ , is given by

$$R = \{(i, j) \mid (i, j) \in E, f_{ij} < c_{ij} \text{ or } (j, i) \in E, f_{ji} > 0\}. \quad (3)$$

Each of the residual arcs has a *residual capacity* given by  $c'_{ij} = c_{ij} - f_{ij}$  if  $(i, j) \in E$  or  $c'_{ij} = f_{ji}$  if  $(j, i) \in E$ . The *maximum flow* problem refers to finding a feasible flow which maximizes the total flow from the source to the sink.

Finally, an *s-t cut* refers to partition of the nodes into two disjoint sets  $S$  and  $T$  such that  $s \in S$  and  $t \in T$ . The sets  $S$  and  $T$  are referred to as the source and sink sets, respectively. The *minimum cut* problem, which is the dual of the maximum flow problem, refers to finding an *s-t cut* which minimizes the sum of capacities for the arcs going from  $S$  to  $T$ .

### 2.1 Augmenting Paths

The augmenting paths (AP) family of min-cut/max-flow algorithms is the oldest of the three families and was introduced with the Ford-Fulkerson algorithm [18]. AP algorithms always maintain a

1. I.e. the implementation released by the authors.

feasible flow and work by pushing flow along so-called *augmenting paths*, which are paths from  $s$  to  $t$  in the residual graph. Pushing flow along a path refers to adding a flow,  $f$ , to the flow value,  $f_{ij}$ , for each arc,  $(i, j)$ , along the path. To maintain a feasible flow, the maximum flow that can be pushed is equal to the minimum residual capacity along the path. The algorithms terminate when no more augmenting paths can be found.

The primary difference between various AP algorithms lies in how the augmenting paths are found. For computer vision applications, the most popular AP algorithm is the Boykov–Kolmogorov (BK) algorithm [9], which works by building search trees from both the source and sink nodes to find augmenting paths and uses a heuristic that favors shorter augmenting paths. The BK algorithm has great performance in practice, but the theoretical run time bound is worse than other algorithms [62].

In terms of performance, the BK algorithm has been surpassed by the Incremental Breadth First Search (IBFS) algorithm by Goldberg et al. [26]. The main difference between the two algorithms is that IBFS maintains the source and sink search trees as breadth-first search trees, which results in both a better theoretical run time and better practical performance [26, 25].

## 2.2 Preflow Push-Relabel

The second family of algorithms are the preflow push-relabel (PPR) algorithms, which were introduced by Goldberg and Tarjan [24]. These algorithms do *not* maintain a feasible flow but instead use a so-called *preflow*, which satisfies capacity constraints but allows nodes to have more incoming than outgoing flow (thereby violating conservation constraints). The difference between the incoming and outgoing flow for a node,  $i$ , is denoted as its *excess*,  $e_i \geq 0$ . Moreover, PPR algorithms maintain a labelling,  $d_i$ , for every node. If  $d_i < n$ , it is a lower bound on the distance from node  $i$  to  $t$ . If  $d_i \geq n$ , the sink cannot be reached from this node and  $n - d_i$  then gives a lower bound on the distance to  $s$ . Labels for  $s$  and  $t$  remain fixed at  $n$  and 0, respectively.

PPR algorithms work by repeatedly applying one of two actions [13, 24]: *push* and *relabel*. The *push* operation selects a node with positive excess and pushes flow to a neighbor node with a label of lower value. If no neighbor has a lower label, the *relabel* operation is used to increase the label of a node by one. The algorithms terminate when no nodes with positive excess have a label  $d_i < n$ , which means that no more flow can be pushed to the sink. At this point, the minimum  $s$ - $t$  cut can be extracted, by inspecting the node labels. If  $d_i \geq n$  then  $i \in S$ , otherwise  $i \in T$ . Extracting the maximum flow requires an extra step, since the preflow may not be a valid flow. However, this work is generally a small part of the run time [62] and for computer vision applications we are typically only interested in the minimum cut anyway.

The difference between various PPR algorithms lies in the order in which push and relabel operations are performed. Early variants used simple heuristics, such as always pushing flow from the node with the highest label or using a first-in-first-out queue to keep track of nodes with positive excess [11]. More recent versions [3, 22, 23] use sophisticated heuristics and a mix of local and global operations to obtain significant performance improvements over early PPR algorithms.

## 2.3 Pseudoflow

The most recent family of min-cut/max-flow algorithms is the pseudoflow family, which was introduced with the Hochbaum

pseudoflow (HPF) algorithm [30, 31]. These algorithms use a so-called *pseudoflow* and, like the PPR algorithms, do not maintain a feasible flow. A pseudoflow satisfies capacity constraints but not the conservation constraints, as it has no constraints on the difference between incoming and outgoing flow. As with preflow, we refer to the difference between incoming and outgoing flow for a node as its excess,  $e_i$ . A positive excess is referred to as a *surplus* and a negative excess as a *deficit*. The difference between pseudoflow and preflow is that preflow only allows non-negative excesses.

Pseudoflow algorithms can be seen as a hybrid between AP and PPR algorithms. They maintain a forest of trees, where each node with a surplus or deficit is the root of a tree and all roots must have a surplus or deficit. Let  $\mathcal{S}$  and  $\mathcal{T}$  denote the forests of trees rooted in  $s$  and  $t$ , respectively. In each iteration, the algorithms grow these trees by adding nodes with zero excess until an arc,  $a$ , connects a tree from  $\mathcal{S}$  to a tree from  $\mathcal{T}$ . This new path from  $s$  to  $t$  through  $a$  is an augmenting path and flow is pushed along it. In contrast to AP algorithms, the only restrictions on how much flow to push are the arc capacities, since pushing flow is allowed to create new deficits or surpluses. If it is not possible to grow a tree — either by adding a free node or finding a connection to a tree in the other forest — the algorithms terminate. As with PPR algorithms, only the minimum cut can be extracted at this point and additional processing is needed to access the maximum flow.

There are two main algorithms in this family: HPF and Excesses Incremental Breadth First Search (EIBFS) [25]. The main differences are the order in which they scan through nodes when looking for an arc connecting  $\mathcal{S}$  and  $\mathcal{T}$ , and how they push flow along augmenting paths. Both have sophisticated heuristics for these choices, which makes use of many of the same ideas developed for PPR algorithms — including a distance labelling scheme to select which nodes from each forest to merge.

## 2.4 Implementation Details

As stressed by [62], the implementation details can significantly affect the measured performance of a given min-cut/max-flow algorithm. In this section, we will highlight the trends of modern implementations and how they differ.

### 2.4.1 Data Structures

The implementations considered in this paper all use a variant of the adjacency list structure [14] to represent the underlying graph. The most common setup mimics the BK algorithm and is similar to the doubly connected edge list<sup>2</sup> [5]. There is a list of nodes and a list of directed (half-)arcs. Each Node structure stores a pointer to its first outgoing half-arc. Each Arc stores a pointer to the node it points to, a pointer to the next outgoing arc for the node it points from, a pointer to its reverse arc, and a residual capacity. For algorithms developed with computer vision applications in mind (e.g. BK, IBFS, EIBFS) each node also stores a source and sink capacity and now arcs are actually connected to the terminal nodes. Other algorithms simply keep track of which nodes are the source and sink, and then only use Arcs. HPF also differs in that it stores double arcs with a capacity, flow, and direction. It also common to store auxiliary values such as excesses, labels, or more.

As a result of these differences, the Arc and Node data structures used for these lists vary between implementations as

2. Also known as the half-edge data structure.

demonstrated by the differences in the size of the data structures listed in Table 1. For all of the implementations we consider, the memory footprint of the graph correlates linearly with the size of the `Arc` and `Node` data structures. Thus, the size of these structures significantly impact the memory footprint of the graph, which in many cases also influences performance due to the way the CPU fetches and caches data from memory. For these reasons it is generally beneficial to keep the data structures small. Note that some compilers do not pack data structures densely by default, which may significantly increase the size of the `Arc` and `Node` data structures.

#### 2.4.2 Indices vs. Pointers

One way to reduce the size of the `Arc` and `Node` data structures on 64-bit system architectures is to use indices rather than pointers to reference nodes and arcs. As long as the indices can be stored using unsigned 32-bit integers, we can cut the size of the arc and node references in half by using unsigned 32-bit integers instead of pointers (which are 64-bit). This approach can significantly reduce the size of the `Arc` and `Node` data structures, as the majority of the structures consist of references to other arcs and nodes [36]. The downside to this approach is that extra computations are required every time we need to fetch an arc or a node.

Some grid-based algorithms [36] use 32-bit indices to reduce the size of their data structure. The generic algorithms we have investigated in this work all use pointers to store references between nodes and arcs. Some implementations avoid the extra memory requirement by compiling with 32-bit pointers. However, 32-bit pointers limit the size of the graph much more than 32-bit indices. The reason is that the 32-bit pointers only have 4 GB of address space and the `Node` and `Arc` structures they point to take up many bytes. For example, the smallest `Arc` structure we have tested, *c.f.* Table 1, uses 24 bytes, meaning an implementation based on 32-bit *indices* could handle graphs with 24 times more arcs than one based on 32-bit *pointers*.

#### 2.4.3 Arc Packing

The order in which the arcs are stored may impact the performance significantly. *Arc packing* is used to reduce CPU cache misses, by storing the arcs in the same order that they will be accessed by the algorithm. For instance, min-cut/max-flow algorithms often iterate over outgoing arcs from a node, which makes it beneficial to store outgoing arcs from the same node adjacent in memory. However, as arcs may be added to the graph in any order, packing the arcs usually incurs an overhead from maintaining the correct ordering or reordering all arcs as an extra step before computing the min-cut/max-flow. Similar to arc packing, *node packing* may improve performance. However, this is not done in practice as opposed to arc packing.

Of the previous implementations we examined, only HI-PR [13], IBFS, and EIBFS implement arc packing. These all implement it as an extra step, where arcs are reordered after building the graph but before the min-cut/max-flow computations start. None of the examined implementations use node packing.

#### 2.4.4 Arc Merging

In practice, it is not uncommon that multiple arcs between the same pair of nodes are added to the graph. Merging these arcs into a single arc with a capacity equal to the sum of capacities of the merged arcs may reduce the graph size significantly. As this decreases both the memory footprint of the graph as well

as the number of edges to be processed, it can have substantial performance benefits [36, 59]. However, as redundant arcs can usually be avoided by careful graph construction and they should have approximately the same performance impact on all algorithms, we have not investigated the effects of this further.

### 3 PARALLEL MIN-CUT/MAX-FLOW

Like serial algorithms, parallel algorithms for min-cut/max-flow problems can be split into families based on shared characteristics. A key characteristic is whether the algorithms parallelize over individual graph nodes (node-based parallelism) or split the graph into sub-graphs that are then processed in parallel (block-based parallelism). Other important algorithmic traits include whether the algorithm is distributed, which we are not concerned with in this paper, and the guarantees in terms of convergence, optimality, and completeness provided by the algorithm.

We should note that since many (but not all) min-cut/max-flow problems in computer vision are defined on grid graphs, several algorithms [35, 36, 57, 63] have exploited this structure to create very efficient parallel implementations. There are, however, many important computer vision algorithms that are not defined on grid graphs, so in this paper we only consider generic min-cut/max-flow algorithms.

The category of node-based parallel algorithms is generally dominated by parallel versions of PPR algorithms. In the block-based category, we have identified three main approaches: adaptive bottom-up merging, dual decomposition, and region discharge, which we investigate. In the following sections, we give an overview of each approach and briefly discuss its merits and limitations.

#### 3.1 Parallel Preflow Push-Relabel

PPR algorithms have been the target of most parallelization efforts [2, 4, 6, 15, 21, 32, 63], since both push and relabel are local operations, which makes them well suited for parallelization. Because the operations are local, the algorithms generally parallelize over each node — performing pushes and relabels concurrently. To avoid data races during these operations, PPR algorithms either use locking [2] or atomic operations [32]. As new excesses are created, the corresponding nodes are added to a queue, from which threads can poll them. In [6], a slightly different approach is applied, where pushes are performed in parallel, but excesses and labels are updated later in a separate step, rather than immediately after the push.

Since parallel PPR algorithms parallelize over every node, they can achieve good speed-ups and scale well to modern multi-core processors [6], or even GPUs [63]. However, synchronization overhead means that many threads are needed to achieve good performance compared to an efficient serial algorithm [6]. As Ahmdahl’s Law [1] dictates, the speed-up from using more computational threads depends on how much of the computation is done in parallel. Therefore, when threads are waiting for synchronization, no parallel work is done which reduces the speed-up. As a result, these algorithms have not achieved dominance outside of large grid graphs for min-cut/max-flow problems [69].

#### 3.2 Adaptive Bottom-Up Merging

The adaptive bottom-up merging approach introduced by Liu and Sun [49] uses block-based parallelism and has two phases, which are summarized in Fig. 1. In phase one, the graph is partitioned

into a number of disjoint sets (blocks) and arcs between blocks have their capacities set to 0 — effectively removing them from the graph. For each pair of blocks connected by arcs, we store a list of the connecting arcs (with capacities now set to 0) along with their original capacities. Disregarding  $s$  and  $t$ , the nodes in each block now belong to disjoint sub-graphs and we can compute the min-cut/max-flow solution for each sub-graph in parallel. The min-cut/max-flow computations are done with the BK algorithm — although one could in theory use any min-cut/max-flow algorithm.

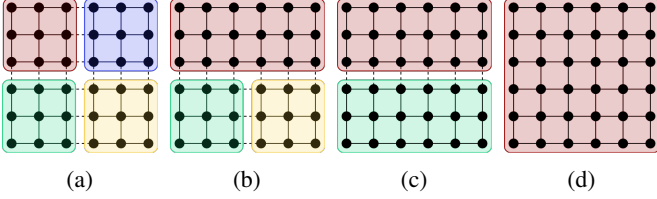


Fig. 1: Illustration of the adaptive bottom-up merging approach for parallel min-cut/max-flow. Terminal nodes and arcs are not shown. Note that the underlying graph does *not* have to be a grid graph. Phase one: (a) The graph is split into blocks and the min-cut/max-flow is computed for each block in parallel. Phase two: (b) The topmost blocks are locked, merged, and the min-cut/max-flow recomputed. (c) As the topmost block is locked, the next thread works on the bottom-most blocks (in parallel). (d) Last two blocks are merged and min-cut/max-flow recomputed to achieve the globally optimal solution.

In phase two, we merge the blocks to get the complete globally optimal min-cut/max-flow. To merge two blocks, we restore the arc capacities for the connecting arcs and then recompute the min-cut/max-flow for the combined graph. This step makes use of the fact that the BK algorithm can reuse its internal search trees [42] to efficiently recompute the min-cut/max-flow when small changes are made to the residual graph for a min-cut/max-flow solution.

For merges in phase two to be performed in parallel, the method marks the blocks being merged as locked. The computational threads then scan the list of block pairs, which were originally connected by arcs, until they find a pair of unlocked blocks. The thread then locks both blocks, performs the merge, and unlocks the new combined block. To avoid two threads trying to lock the same block, a global lock prevents more than one thread from scanning the list of block pairs at a time.

As the degree of parallelism decreases towards the end of phase two — since there are few blocks left to merge — performance increases when computationally expensive merges are performed early in phase two. To estimate the cost of merging two blocks, [49] uses a heuristic based on the potential for new augmenting paths to be formed by merging two blocks. This heuristic determines the merging order of the blocks.

By using block-based, rather than node-based parallelism, adaptive bottom-up merging avoids much of the synchronization overhead that the parallel PPR algorithms suffer from. However, its performance depends on the majority of the work being performed in phase one and in the beginning of phase two, where the degree of parallelism is high.

### 3.3 Dual Decomposition

The dual decomposition (DD) approach was introduced by Strandmark and Kahl [60] and later refined by Yu et al. [68, 69]. Their

algorithm works as follows: first, the nodes of the graph are divided into a set of overlapping blocks (see Fig. 2(a)). Then, the graph is split into disjoint blocks, where the nodes in the overlapping regions are duplicated in each block (see Fig. 2(b)). It is important that the blocks overlap such that if node  $i$  is connected to node  $j$  in block  $b_j$  and node  $k$  in block  $b_k$ , then  $i$  is also both blocks  $b_j$  and  $b_k$ .

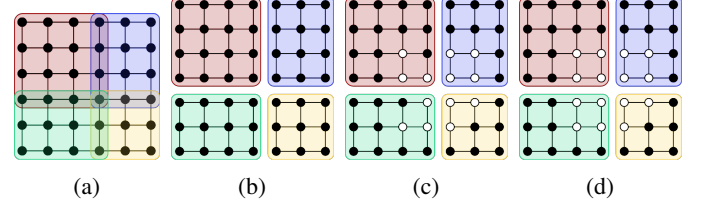


Fig. 2: Illustration of the dual decomposition approach. Terminal nodes and arcs are not shown. Note that the underlying graph does *not* have to be a grid graph. (a) Graph nodes are divided into a set of overlapping blocks. (b) The graph is split into disjoint sub-graphs and nodes in overlapping regions are duplicated into each block. (c) The min-cut/max-flow for each block is computed in parallel which gives an assignment to source set (black) or sink set (white). The source/sink capacities are then adjusted for disagreeing duplicated nodes. (d) The min-cut/max-flow is recomputed and capacities are adjusted until all duplicated nodes agree.

Once the graph has been partitioned into overlapping blocks, the algorithm proceeds iteratively. First, the min-cut/max-flow for each disjoint block is computed in parallel using the BK algorithm. Next, for each duplicated node it is checked if all duplicates of that node are in the same  $s$ - $t$  partitioned set,  $S$  or  $T$ . In that case, we say that the node duplicates agree on their assignment. If all duplicated nodes agree on their assignment, the computed solution is the globally optimal one and the algorithm terminates. If not, the terminal arc capacities for the disagreeing duplicated nodes are updated according to a supergradient<sup>3</sup> ascent scheme and the min-cut/max-flow is recomputed. This process of updating terminal capacities and recomputing the min-cut/max-flow is repeated until all duplicated nodes agree on their assignment.

A limitation of the original dual decomposition approach is that convergence is not guaranteed. Furthermore, [69] and [59] have demonstrated that the risk of nonconvergence increases as the graph is split into more blocks. To overcome this, Yu et al. [69] introduced a new version with a simple strategy that guarantees convergence: if the duplicated nodes in two blocks do not belong to the same set,  $S$  or  $T$ , after a fixed number of iterations, the blocks are merged and the algorithm continues. This trivially guarantees convergence since, in the worst case, all blocks will be merged, at which point the global solution will be computed serially. However, performance significantly drops when merging is needed for the algorithm to converge, as merging only happens after a fixed number of iterations and all blocks may (in the worst case) have to be merged for convergence.

### 3.4 Region Discharge

The region discharge approach was introduced by Shekhovtsov and Hlaváč [59], who generalized earlier work by Delong and Boykov [15]. The method first partitions the graph into a set of blocks

3. Analogous to subgradients for convex functions [8].

(called regions in [59]). Each block  $R$  has an associated *boundary* defined as the set of nodes

$$B^R = \{v \in V \mid v \notin R, (u, v) \in E, u \in R, v \neq s, t\}. \quad (4)$$

Capacities for arcs going from a boundary node to a block node are set to zero. This means that flow can be pushed *out* of the region into the boundary, but not vice versa. Furthermore, each node is allowed to have an excess.

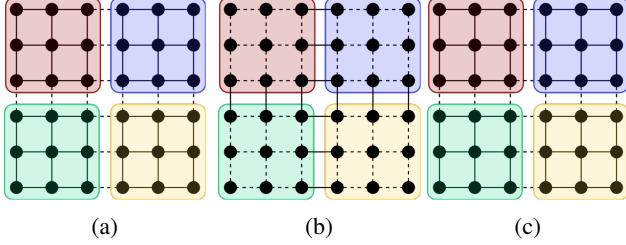


Fig. 3: Illustration of the region discharge approach. Terminal nodes and arcs are not shown. Note that the underlying graph does *not* have to be a grid graph. (a) Graph nodes are divided into a set of blocks, then the region discharge operation is run on each block which pushes flow to the sink or boundary nodes. (b) Flow is synchronized between boundary nodes. (c) Region discharge is run again. The process repeats until no flow crosses the block boundaries.

The method then makes of the *region discharge* operation, which aims to push as much excess flow to the sink or the boundary nodes as possible (the source,  $s$ , is assumed to have an infinite excess). In [59], they use a PPR algorithm or an AP algorithm (specifically, BK) for this purpose. When using a PPR algorithm, the discharge of a block is done by only performing push and relabel operations on nodes in the blocks. When using the BK algorithm, excesses are modelled as arcs from the source, and the possibility to create excess in a node is modelled by adding an infinite capacity arc from the node to the sink. Since arcs leaving the boundary have been set to zero, flow can now only be pushed to the sink or the boundary nodes and the AP algorithm is run as normal.

The discharge operation is performed on each block in parallel. Afterwards, flow along boundary arcs is synchronized between neighboring blocks. This may create additional excesses in some blocks, since boundary nodes overlap with another block. The process of discharge and synchronization is repeated until no new excesses are created, at which point the algorithm terminates. It is proved in [59] that this process will terminate in a finite number of iterations.

The guarantee of convergence, without having to merge blocks, is beneficial, as it means the algorithm can maintain a high degree of parallelism while computing the min-cut/max-flow solution. However, because flow must be synchronized between blocks, the practical performance of the method still depends on well-chosen blocks and may be limited by synchronization overhead. For details on the heuristics used in the algorithm, which are also important for its practical performance, see [59].

## 4 PERFORMANCE COMPARISON

We now compare the performance of the algorithms discussed in the previous sections. For all experiments, the source code

was compiled with the GCC C++ compiler version 9.2.0 with `-O3` optimizations on a 64-bit Linux-based operating system with kernel release 3.10. Experiments were run on a dual socket NUMA<sup>4</sup> system with two Intel Xeon Gold 6226R processors with 16 cores each and HTT<sup>5</sup> disabled, for a total of 32 parallel CPU threads. The system has 756 GB of RAM and for all experiments all data was kept in memory. For the parallel algorithm benchmarks, we ensure that cores are allocated on the same socket and memory is allocated on local RAM where possible.

Run times were measured as the minimum time over three runs and no other process (apart from the OS) were running during the benchmarks. We split our measured run time into two distinct phases: build time and solve time. Build time refers to the construction of the graph and any additional data structures used by an algorithm. If the algorithm performs arc packing or similar steps, this is included in the build time. To ensure the build time is a fair representation of the time used by an algorithm, we precompute a list of nodes and arcs and load these lists fully into memory before starting the timing. Solve time refers to the time required to compute the min-cut/max-flow. For algorithms, such as PPR, that only compute a minimum cut, we do not include the time to extract the full maximum flow solution. The reason for this is that for most computer vision applications the minimum cut is of principal interest. Furthermore, converting to a maximum flow solution usually only adds a small overhead [62].

### 4.1 Datasets

We test the algorithms on the commonly used benchmark dataset published by the University of Waterloo [51]. This dataset includes a variety of computer vision problems, such as stereo matching, image segmentation, multi-view reconstruction, and surface fitting. Furthermore, our experiments include the super resolution, texture restoration, deconvolution, decision tree field (DTF), and automatic labelling environment (ALE) datasets from [62]. Finally, we include problems from two recent papers [37, 39] which perform multi-object image segmentation via surface fitting. Note that some datasets consist of many small problem instances which must be run in sequence. For these, we report the accumulated times. All benchmark data is available at DOI:10.5281/zenodo.4905882 [52].

For the parallel algorithm benchmarks, we only include a subset of all datasets. The reason for this is that parallelization is mainly of interest for large problems with long solve times. For the same reasons, we exclude datasets consisting of many small problem instances. For the block-based algorithms, we split the graph into blocks in one of the following ways:

- 1) For graphs based on an underlying image grid, we define blocks by recursively splitting the image grid along its longest axis until we have the required number of blocks.
- 2) For the surface based segmentation methods [37, 39], we first define blocks such that nodes associated with a surface are in their own block. We then merge blocks with their nearest neighbor based on the centroids of the initial surfaces until we have the required number of blocks.

For the bottom-up merging, we always use 64 blocks (two times the maximum thread count) — except for the datasets from [39] where we use two blocks per object. For dual decomposition and region discharge, we use one block per thread.

4. Non-Uniform Memory Access  
5. Hyper-Threading Technology



## 4.2 Tested Implementations

All of the tested implementations are available at [github.com/patmjmen/maxflow\\_algorithms](https://github.com/patmjmen/maxflow_algorithms) and are archived at DOI:10.5281/zenodo.4912409 [38].

**BK** [9] We test the reference implementation (BK) of the Boykov-Kolmogorov algorithm from <http://pub.ist.ac.at/~vnk/software.html>. Furthermore, we test our own implementation of BK (MBK), which contains several optimizations. Most notably, our version uses indices instead of pointers to reduce the memory footprint of the `Node` and `Arc` data structures. Finally, we test a second version (MBK-R), which reorders arcs such that all outgoing arcs from a node are adjacent in memory. This increases cache efficiency but uses more memory and requires an extra initialization step.

**EIBFS** [25] We test a slightly modified version [33] (**EIBFS**) of the excesses incremental breadth first search algorithm originally implemented by [25] available from <https://github.com/sydbarrett/AlphaPathMoves>. This version uses slightly bigger data structures to support non-integer arc capacities and larger graphs, compared to the implementation tested in [25]. Although these changes may decrease performance slightly, we think it is reasonable to use the modified version, as several of the other algorithms have similar sacrifices in terms of performance. Additionally, we test our own modified version of EIBFS (EIBFS-I), which replaces pointers with indices to reduce the memory footprint. Finally, as both EIBFS and EIBFS-I performs arc reordering during initialization, we also test a version without arc reordering (EIBFS-I-NR) to better compare with other algorithms.

**HPF** [30] We test the reference implementation of Hochbaum pseudoflow (HPF) from <https://riot.ieor.berkeley.edu/Applications/Pseudoflow/maxflow.html>. This implementation has four different configurations that we test:

- 1) Highest label with FIFO buckets (HPF-H-F).
- 2) Highest label with LIFO buckets (HPF-H-L).
- 3) Lowest label with FIFO buckets (HPF-L-F).
- 4) Lowest label with LIFO buckets (HPF-L-L).

**HI-PR** [13] We test the implementation of the preflow push-relabel algorithm from [https://cmp.felk.cvut.cz/~shekhovt/d\\_maxflow/index.html](https://cmp.felk.cvut.cz/~shekhovt/d_maxflow/index.html)<sup>6</sup>.

**P-ARD** [59] We test the implementation of parallel augmenting paths region discharge (P-ARD) from [https://cmp.felk.cvut.cz/~shekhovt/d\\_maxflow/index.html](https://cmp.felk.cvut.cz/~shekhovt/d_maxflow/index.html). P-ARD is an example of the region discharge approach.

**Liu-Sun** [49] Since no public reference implementation is available, we test our own implementation of the adaptive bottom-up merging approach based on the paper by Liu and Sun [49].

**P-PPR** [6] We test the implementation of a recent parallel preflow push-relabel algorithm from <https://github.com/niklasb/pbbs-maxflow>.

**Strandmark-Kahl** [60] We test our own implementation of the Strandmark-Kahl dual decomposition algorithm based on the implementation at [https://cmp.felk.cvut.cz/~shekhovt/d\\_maxflow/index.html](https://cmp.felk.cvut.cz/~shekhovt/d_maxflow/index.html)<sup>7</sup>. The original implementation can only handle grid graphs with rectangular blocks, while our implementation can handle arbitrary graphs and arbitrary blocks at the cost of some

additional overhead during graph construction. Note that our implementation does not implement the merging strategy proposed by [69] and therefore is not guaranteed to converge. We only include results for cases where the algorithm does converge.

Table 1 lists the tested implementations along with their type and memory footprint. Their memory footprint can be calculated based on the number of nodes and arcs in the graph and will be discussed further in Section 5.

TABLE 1: Summary of the tested implementations including their memory footprint. The table shows the bytes required per node and per arc assuming 32-bit indices where applicable. For arcs, the reported size includes both forward and backward arcs, since some implementations store these in a single data structure. These numbers depend on, but are *not* the same as, the `Node` and `Arc` structure sizes, as the footprint reported here includes all data structures used by the algorithm

Serial algorithms	Algorithm type	Node	Arc
HI-PR <sup>a</sup> [13]	Preflow push-relabel	40 B	40 B
HPF <sup>b</sup> [30]	Pseudoflow	96 B	25 B
EIBFS [25]	Pseudoflow		
↳EIBFS <sup>c</sup>	Pseudoflow	72 B	72 B
↳EIBFS-I*	Pseudoflow	29 B	50 B
↳EIBFS-I-NR*	Pseudoflow	29 B	24 B
BK [9]	Augmenting path		
↳BK <sup>d</sup>	Augmenting path	44 B	64 B
↳MBK*	Augmenting path	23 B	24 B
↳MBK-R*	Augmenting path	23 B	48 B
Parallel algorithms			
P-PPR <sup>e</sup> [6]	Parallel preflow push-relabel	48 B	68 B
Liu-Sun* [49]	Adaptive bottom-up merging <sup>†</sup>	25 B	24 B
Strandmark-Kahl* [60]	Dual decomposition <sup>†</sup>	29 B	24 B
P-ARD <sup>a</sup> [59]	Region discharge <sup>†</sup>	40 B	32 B

<sup>†</sup>Uses BK (augmenting path).

\*Implemented or updated by us: [https://github.com/patmjmen/maxflow\\_algorithms](https://github.com/patmjmen/maxflow_algorithms)

<sup>a</sup>[https://cmp.felk.cvut.cz/~shekhovt/d\\_maxflow/index.html](https://cmp.felk.cvut.cz/~shekhovt/d_maxflow/index.html)

<sup>b</sup><https://riot.ieor.berkeley.edu/Applications/Pseudoflow/maxflow.html>

<sup>c</sup><https://github.com/sydbarrett/AlphaPathMoves>

<sup>d</sup><http://pub.ist.ac.at/~vnk/software.html>

<sup>e</sup><https://github.com/niklasb/pbbs-maxflow>

## 4.3 Serial Algorithms

### 4.3.1 Overall Performance

The primary experimental results for the serial algorithms are listed in Table 2. The table shows the results for each algorithm. When several different implementations were tested, only the fastest variant is shown. The results from Table 2 are summarized in Fig. 5, which shows the distribution of the solve time and the total time for each algorithm on each dataset relative to the fastest algorithm on the dataset. Thus, for a given dataset, a relative performance score of 0.5 means that the algorithm was half as fast as the fastest algorithm on that dataset. The distribution of these scores then gives a clear indication of how well the different algorithms perform relative to each other.

From Fig. 5(b), we see that EIBFS and HPF outperform the two other algorithms on the majority of the datasets in terms of the solve time. Both algorithms have their upper quartiles equal to 1, meaning that they had the fastest solve time for at least 25% of the datasets. As indicated by the median, EIBFS had the fastest solve time for almost half of the datasets, while HI-PR was about five times slower than the fastest algorithm for over half of the datasets.

<sup>6</sup> Originally from <http://www.avglab.com/andrew/soft.html>, but the link is no longer available.

<sup>7</sup> Originally from <https://www1.maths.lth.se/matematiklth/personal/petter/cppmaxflow.php> but the link is no longer available.

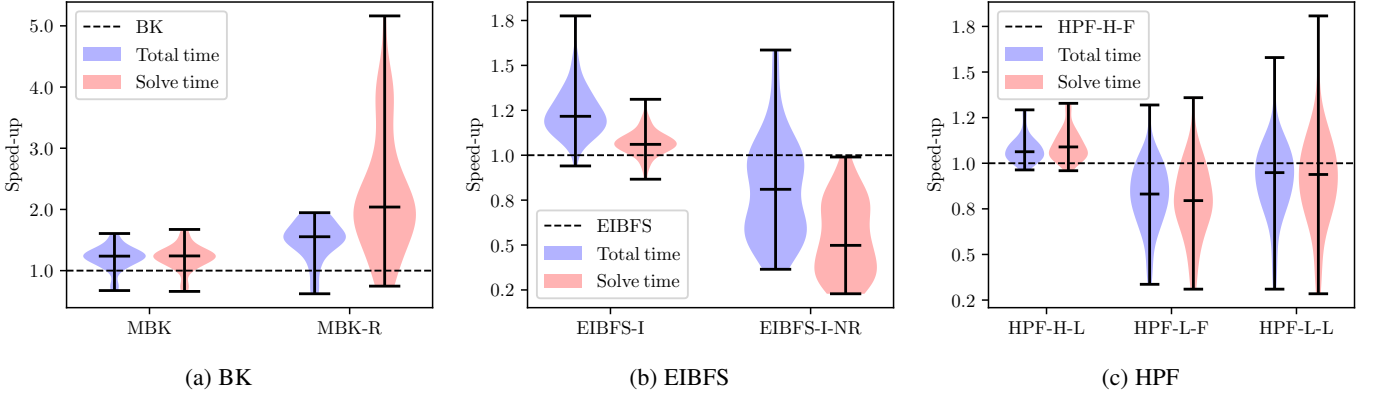


Fig. 4: Performance comparison of serial algorithm variants. The solve time and total time is compared against the times for the chosen reference algorithm for each dataset.

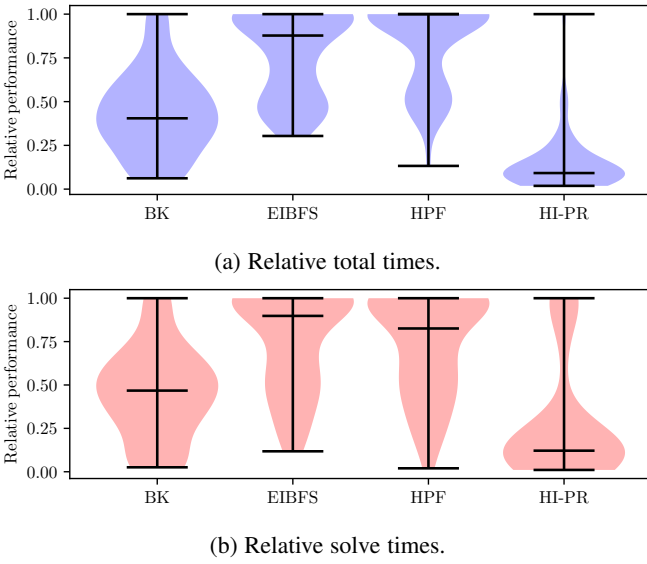


Fig. 5: Relative performance for the serial algorithms. For each dataset, the solve and total times for each algorithm were compared to those of the fastest algorithm for that dataset and a relative time was computed. This shows how often an algorithm was fastest and, if it was not fastest, how much slower than the fastest it was.

We see that all four algorithms have cases where they are over four times slower than the fastest algorithm in terms of solve time, and that HPF has slightly better worst case performance than EIBFS. Note also the bimodality of the distributions for EIBFS and HPF which shows that they either performed best (or close to it) or they were about half as fast as the best one.

While EIBFS generally has the fastest solve times, Fig. 5(a) shows that HPF has the fastest total time (build time + solve time) for the majority of the datasets, as indicated by a median relative performance equal to 1. Furthermore, HPF performs consistently well across all datasets and rarely drops below 0.5 in relative performance compared to the fastest algorithm while staying above 0.7 for three out of four datasets. Again, EIBFS and HPF show a bimodality near the top and at 0.5. BK maintains similar relative performance as for solve time, being around half as fast as the fastest algorithm for the majority of the datasets. Meanwhile HI-PR falls even further behind compared to the results for solve time,

with an upper quartile below 0.2 in relative performance, which means that it is at least five times slower than the fastest algorithm for three out of four datasets.

#### 4.3.2 Algorithm Variants

The different variants of each algorithm are compared in Fig. 4, which shows the relative performance of each implementation compared to a chosen “reference” implementation. For the BK algorithm, the BK implementation is used for reference, for the EIBFS algorithm, the EIBFS implementation is used as a reference, and for HPF the highest label FIFO configuration is used as reference, since it is the one recommended by the authors. As we are now measuring relative to a specific implementation, rather than the fastest one as we did in Fig. 5, it is possible to get a relative performance score of more than one.

For the BK algorithms, both MBK and MBK-R outperform BK for the vast majority of the datasets. MBK is consistently faster than BK, while MBK-R outperforms MBK for most of the datasets. Although MBK-R outperforms the two other variants, its relative speed-up decreases significantly when measured on total time versus just solve time. This clearly reflects the effect of arc packing (reordering the arcs), in that it typically decreases solve at the cost of increased build time.

The EIBFS variants show similar results to BK, with our index-based version (EIBFS-I) outperforming the reference implementation consistently showing over 20% improved performance for the majority of the datasets and only a few instances with slightly lower performance than EIBFS. Meanwhile, EIBFS-I-NR performs worse than EIBFS on almost all datasets, which further supports the notion that arc packing is important for the performance of the implementation.

For the HPF algorithm, the H-LIFO configuration (HPF-H-L) consistently performs the best, while the L-FIFO and L-LIFO configurations perform worse than the reference H-FIFO configuration for the majority of datasets. Although there are a few cases where L-LIFO performs much better than the others, it generally performs much worse than both H-LIFO and H-FIFO.

#### 4.4 Parallel Algorithms

Our benchmark results for the parallel algorithms are shown in Table 3, where we compare the build and solve time for each algorithm on each dataset. As mentioned, we do not include results



TABLE 2: Performance comparison of serial algorithms based on both their solve and total (build + solve) times. Datasets have been grouped according to their problem family. Only the fastest variant of each algorithm (measured in total time) is included and the same variant was used for all datasets. The fastest solve time for each dataset has been underlined and the fastest total time has been marked with **bold face**

Dataset	Nodes	Arcs	MBK-R [9]		EIBFS-I [25]		HPF-H-L [30]		HI-PR [13]	
			Solve	Total	Solve	Total	Solve	Total	Solve	Total
Multi-view										
BL06-camel-lrg	18 M	93 M	107.53 s	111.42 s	28.55 s	31.54 s	24.44 s	28.82 s	291.71 s	337.91 s
BL06-gargoyle-lrg	17 M	86 M	238.08 s	241.65 s	33.76 s	36.57 s	26.51 s	30.61 s	208.27 s	251.10 s
3D Segmentation: surface-based										
NT32_tomo3_raw_10	22 M	154 M	52.86 s	63.15 s	50.82 s	60.01 s	36.46 s	44.14 s	645.33 s	741.98 s
NT32_tomo3_raw_100	183 M	1 B	778.39 s	860.71 s	553.50 s	627.08 s	520.26 s	583.76 s	9732.34 s	10618.81 s
NT32_tomo3_raw_3	7 M	49 M	15.42 s	18.69 s	24.22 s	27.19 s	15.87 s	18.33 s	176.11 s	200.29 s
NT32_tomo3_raw_30	67 M	462 M	145.23 s	176.37 s	194.79 s	221.90 s	179.82 s	202.73 s	2939.04 s	3260.63 s
NT32_tomo3_raw_5	11 M	75 M	23.92 s	28.84 s	42.13 s	46.54 s	30.62 s	34.37 s	286.58 s	326.86 s
cells.sd2	3 M	30 M	9.87 s	12.30 s	5.36 s	6.57 s	3.38 s	4.92 s	19.49 s	33.81 s
cells.sd3	13 M	126 M	48.23 s	59.03 s	35.24 s	40.66 s	15.52 s	21.84 s	98.25 s	167.56 s
foam.subset.r120.h210	8 M	113 M	3.12 s	11.90 s	1.71 s	6.80 s	9.25 s	14.20 s	8.26 s	72.93 s
foam.subset.r160.h210	15 M	205 M	6.05 s	22.02 s	3.21 s	12.52 s	17.14 s	26.18 s	15.16 s	145.58 s
foam.subset.r60.h210	1 M	24 M	0.62 s	2.58 s	0.39 s	1.49 s	1.98 s	3.01 s	1.85 s	12.82 s
simcells.sd2	903 K	6 M	1.19 s	1.92 s	0.54 s	0.77 s	0.73 s	1.06 s	4.55 s	6.98 s
simcells.sd3	3 M	27 M	9.93 s	12.10 s	2.94 s	4.12 s	3.23 s	4.60 s	21.57 s	33.89 s
3D Segmentation: voxel-based										
adhead.n26c100	12 M	327 M	65.81 s	92.57 s	22.60 s	33.93 s	24.29 s	29.03 s	225.38 s	424.67 s
adhead.n6c100	12 M	75 M	23.88 s	28.03 s	13.23 s	15.85 s	14.13 s	15.87 s	59.65 s	102.84 s
babyface.n26c100	5 M	131 M	82.29 s	92.87 s	30.13 s	34.74 s	54.47 s	56.71 s	183.60 s	228.09 s
babyface.n6c100	5 M	30 M	7.78 s	9.44 s	5.56 s	6.61 s	11.56 s	12.24 s	57.28 s	69.66 s
bone.n26c100	7 M	202 M	9.01 s	25.62 s	9.18 s	16.28 s	4.24 s	7.16 s	68.39 s	173.75 s
bone.n6c100	7 M	46 M	4.09 s	6.65 s	2.74 s	4.35 s	2.30 s	3.36 s	23.66 s	46.71 s
bone_subx.n26c100	3 M	101 M	7.70 s	15.78 s	4.74 s	8.23 s	2.14 s	3.61 s	25.51 s	75.15 s
bone_subx.n6c100	3 M	23 M	4.10 s	5.36 s	2.38 s	3.11 s	1.28 s	1.81 s	10.34 s	21.49 s
liver.n26c100	4 M	108 M	11.78 s	20.41 s	10.49 s	14.20 s	5.72 s	6.50 s	71.88 s	131.00 s
liver.n6c100	4 M	25 M	10.08 s	11.40 s	5.82 s	6.57 s	5.70 s	6.24 s	30.49 s	42.71 s
Deconvolution										
graph3x3	2 K	47 K	9 ms	11 ms	3 ms	3 ms	1 ms	1 ms	1 ms	5 ms
graph5x5	2 K	139 K	62 ms	67 ms	6 ms	9 ms	3 ms	4 ms	2 ms	15 ms
Decision tree field (DTF)										
printed_graph1	20 K	1 M	0.63 s	0.73 s	0.13 s	0.17 s	40 ms	51 ms	51 ms	0.25 s
printed_graph16	11 K	683 K	0.24 s	0.29 s	44 ms	62 ms	16 ms	22 ms	25 ms	0.12 s
Super resolution										
super_res-E1	10 K	62 K	2 ms	4 ms	1 ms	2 ms	2 ms	3 ms	1 ms	7 ms
super_res-E2	10 K	103 K	5 ms	7 ms	2 ms	3 ms	2 ms	3 ms	2 ms	12 ms
super_res-Paper1	10 K	62 K	2 ms	4 ms	1 ms	2 ms	2 ms	3 ms	1 ms	7 ms
superres_graph	43 K	742 K	17 ms	55 ms	10 ms	26 ms	7 ms	12 ms	19 ms	0.16 s
Texture										
texture-Cremer	44 K	783 K	1.54 s	1.58 s	0.35 s	0.37 s	0.17 s	0.19 s	42 ms	0.19 s
texture-OLD-D103	43 K	742 K	0.60 s	0.65 s	0.19 s	0.21 s	73 ms	92 ms	41 ms	0.19 s
texture-Paper1	43 K	742 K	0.65 s	0.69 s	0.19 s	0.21 s	76 ms	95 ms	36 ms	0.17 s
texture-Temp	14 K	239 K	0.22 s	0.23 s	30 ms	34 ms	9 ms	15 ms	6 ms	32 ms
Stereo										
BVZ-sawtooth	164 K	796 K	1.07 s	1.52 s	0.50 s	0.72 s	1.39 s	1.85 s	7.89 s	12.27 s
BVZ-tsukuba	110 K	513 K	0.44 s	0.66 s	0.29 s	0.41 s	0.66 s	0.84 s	4.69 s	6.64 s
BVZ-venus	166 K	795 K	1.93 s	2.48 s	1.10 s	1.36 s	1.94 s	2.46 s	15.00 s	20.11 s
KZ2-sawtooth	294 K	1 M	3.99 s	5.39 s	1.14 s	2.02 s	3.30 s	4.66 s	23.79 s	36.55 s
KZ2-tsukuba	199 K	1 M	2.62 s	3.25 s	0.71 s	1.12 s	1.92 s	2.55 s	20.95 s	27.14 s
KZ2-venus	301 K	2 M	6.20 s	7.77 s	2.18 s	3.16 s	4.70 s	6.21 s	41.63 s	55.60 s
Surface fitting										
LB07-bunny-lrg	49 M	300 M	8.71 s	22.95 s	6.38 s	15.25 s	21.87 s	32.13 s	610.24 s	820.64 s
Automatic labeling environment (ALE)										
graph_2007_000033	174 K	3 M	7.01 s	10.30 s	0.45 s	3.27 s	22.55 s	24.65 s	2.89 s	20.74 s

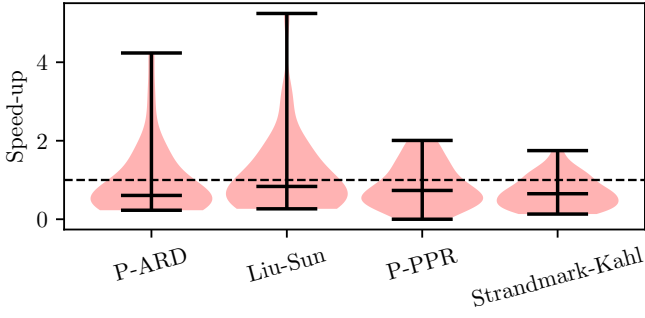


Fig. 6: Speed-up of the parallel algorithms relative to the best serial solve time for each dataset.

for many of the small datasets, as the overhead of parallelization outweighs performance benefits. The table includes the number of CPU threads used by each algorithm for the listed build and solve times. Furthermore, it includes the solve time of the best serial algorithm for each dataset for comparison. To get the complete information, we include the build time in the table. Still, it is the solve time which reveal how successfully the algorithms distribute the work as more threads are added. Additionally, a lack of optimization leads to very long build times for some of the parallel implementations, especially P-PPR and P-ARD, which needs to be taken into consideration when interpreting the results. Finally, it was not possible to run the P-PPR implementation on three of the datasets due to run-time errors and/or memory constraints.

From Table 3, it is clear that no algorithm is dominant. Every algorithm has datasets where it is the fastest and for many of the datasets a serial algorithm gives the best or close to the best performance. The strength of the parallel algorithms lies in the large datasets with over 10 M nodes where significant performance improvements are found. Furthermore, for the datasets where the parallel algorithms are best, Liu-Sun is most often the best performing algorithm.

The superiority of the Liu-Sun algorithm among the parallel algorithms is further illustrated in Fig. 6, which shows that Liu-Sun is faster than the fastest serial algorithm on almost half of the datasets. Moreover, it also has the highest maximum speed-up and often lies close to the best serial algorithm when it does not give better performance. The other parallel algorithms all have median values well below one, or a low maximum speed-up, meaning that they rarely result in a good speed-up compared to the best serial algorithm.

While the parallel algorithms do not outperform the fastest serial algorithm on many of the datasets, it is important to examine which datasets are better suited for the parallel algorithms. Fig. 7 shows the relative speed-up for each algorithm on each dataset compared to the size of each problem, represented by the number of nodes and the fastest serial solve time. The results reinforce that the parallel algorithms perform better for larger datasets, especially P-ARD and Liu-Sun. Interestingly, only P-ARD shows a significant speed-up for small problems.

Finally, Fig. 8 shows the speed-up distribution of the parallel algorithms compared to their single threaded performance. It is clear that the parallel PPR algorithm scales better as the performance consistently improves as more threads are added. For the block-based algorithms, only Liu-Sun shows a consistent

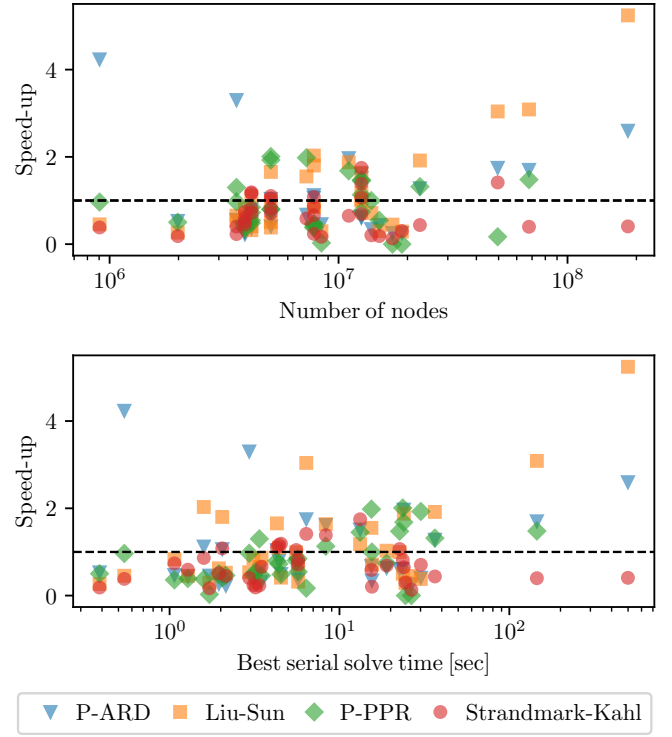


Fig. 7: Plot of the speed-up of the parallel algorithms relative to the problem size. Speed-ups are shown as a function of the number of nodes (top) and best serial solve time (bottom).

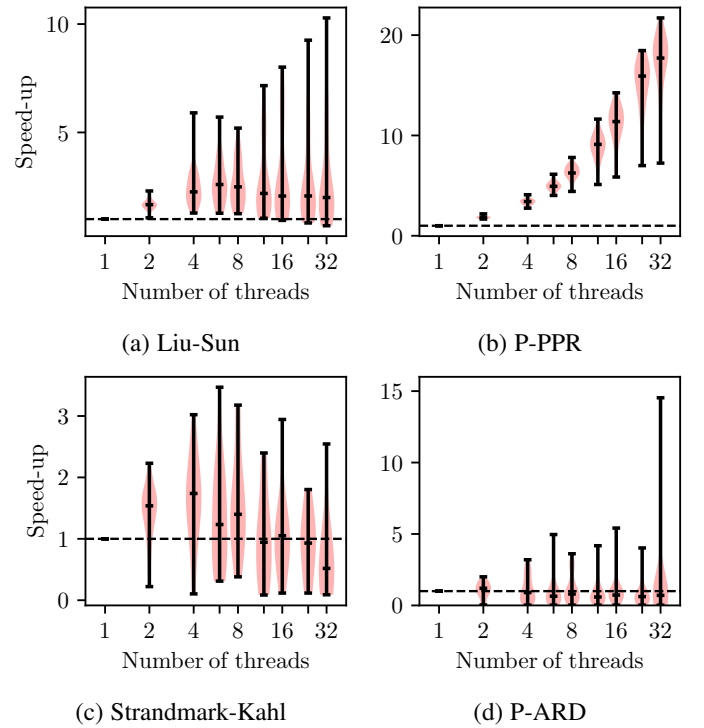


Fig. 8: Speed-up of the the parallel algorithms compared to their single-threaded performance. For each number of threads, the distribution of the speed-ups over all datasets is shown.

TABLE 3: Performance of parallel algorithms based on build and solve times. The parallel algorithms were run with 1, 2, 4, 6, 8, 12, 16, 24, 32, 40, 48, 56, and 64 threads. Only the best time is shown along with the thread count for that run. For comparison, the solve time for the fastest serial algorithm is also included. All times are in seconds. The fastest solve time for each dataset has been marked with **bold face**

Dataset	Nodes	Arcs	Liu-Sun [49]			P-PPR [6]			Strandmark-Kahl [60]			P-ARD [59]		Best serial		
			Build	Best solve		Build	Best solve		Build	Best solve		Build	Best solve	Alg.	Solve	
Multi-view																
BL06-camel-lrg	18 M	93 M	4.04	84.83	16T	-	-	-	1.89	81.28	1T	13.76	95.40	1T	HPF	<b>24.44</b>
BL06-gargoyle-lrg	17 M	86 M	3.73	59.08	4T	-	-	-	1.74	201.29	1T	12.20	102.31	2T	HPF	<b>26.51</b>
3D Segmentation: surface-based																
NT32_tomo3_raw_10	22 M	154 M	5.12	<b>19.02</b>	16T	141.09	27.67	32T	25.42	83.26	2T	26.91	28.45	8T	HPF	36.46
NT32_tomo3_raw_100	183 M	1 B	40.35	<b>95.16</b>	32T	-	-	-	174.91	1226.60	1T	219.76	191.91	16T	HPF	498.94
NT32_tomo3_raw_3	7 M	49 M	1.64	9.94	6T	42.88	<b>7.79</b>	32T	7.44	26.26	1T	6.34	22.81	1T	BK	15.42
NT32_tomo3_raw_30	67 M	462 M	15.28	<b>47.05</b>	32T	430.09	98.17	32T	70.50	364.78	1T	78.17	85.26	6T	BK	145.23
NT32_tomo3_raw_5	11 M	75 M	2.45	12.74	12T	66.34	14.23	32T	12.41	36.80	4T	12.96	<b>12.13</b>	4T	BK	23.92
cells.sd2	3 M	31 M	0.99	5.17	4T	26.79	<b>2.60</b>	32T	3.23	14.62	1T	6.65	6.03	32T	HPF	3.38
cells.sd3	13 M	126 M	3.97	21.78	6T	108.70	15.57	32T	23.90	76.40	1T	21.84	44.98	1T	HPF	<b>15.52</b>
foam.subset.r120.h210	8 M	113 M	3.38	5.83	6T	166.47	63.49	1T	26.72	10.18	1T	18.76	3.74	1T	EIBFS	<b>1.71</b>
foam.subset.r160.h210	15 M	205 M	6.38	10.69	8T	173.13	5.88	32T	52.11	17.24	1T	33.72	7.32	1T	EIBFS	<b>3.21</b>
foam.subset.r60.h210	1 M	24 M	0.75	1.46	8T	20.41	0.77	32T	5.27	2.10	1T	4.16	0.73	1T	EIBFS	<b>0.39</b>
simcells.sd2	903 K	6 M	0.15	1.19	4T	5.47	0.56	32T	0.33	1.42	4T	1.39	<b>0.13</b>	32T	EIBFS	0.54
simcells.sd3	3 M	27 M	0.67	5.49	4T	22.32	3.03	32T	1.47	7.30	6T	4.96	<b>0.89</b>	32T	EIBFS	2.94
3D Segmentation: voxel-based																
adhead.n26c10	12 M	327 M	7.17	<b>18.42</b>	8T	268.67	25.56	12T	26.84	27.50	2T	56.63	29.86	4T	EIBFS	18.94
adhead.n26c100	12 M	327 M	7.22	22.67	8T	262.53	<b>15.33</b>	32T	28.77	21.17	6T	53.39	37.27	8T	EIBFS	22.60
adhead.n6c10	12 M	75 M	1.68	<b>5.08</b>	4T	65.58	7.35	32T	2.46	6.00	2T	13.36	5.14	4T	EIBFS	8.31
adhead.n6c100	12 M	75 M	1.68	11.23	8T	65.84	9.13	32T	2.71	<b>7.57</b>	4T	13.07	8.73	4T	EIBFS	13.23
babyface.n26c10	5 M	131 M	2.98	47.06	4T	102.92	<b>11.74</b>	32T	10.58	28.80	4T	21.15	38.53	2T	EIBFS	23.58
babyface.n26c100	5 M	131 M	3.04	79.04	32T	103.81	<b>15.63</b>	32T	9.95	42.74	4T	22.22	73.55	2T	EIBFS	30.13
babyface.n6c10	5 M	30 M	0.68	<b>2.59</b>	24T	24.96	5.39	24T	0.85	3.88	1T	5.03	4.12	2T	BK	4.28
babyface.n6c100	5 M	30 M	0.68	5.61	4T	24.93	6.93	24T	1.10	<b>5.33</b>	4T	5.37	7.69	2T	EIBFS	5.56
bone.n26c10	7 M	202 M	4.54	3.65	16T	159.32	6.62	32T	15.86	13.15	1T	34.31	8.57	8T	HPF	<b>3.11</b>
bone.n26c100	7 M	202 M	4.52	4.02	32T	158.84	7.65	32T	16.99	5.26	8T	34.22	10.84	8T	HPF	<b>3.48</b>
bone.n6c10	7 M	46 M	1.04	<b>0.78</b>	32T	39.02	4.24	32T	1.46	1.84	2T	7.94	1.41	8T	HPF	1.59
bone.n6c100	7 M	46 M	1.04	<b>1.13</b>	16T	39.15	5.06	32T	1.47	1.89	2T	8.48	1.92	8T	HPF	2.04
bone_subx.n26c10	3 M	101 M	2.36	3.13	16T	78.56	3.90	32T	7.91	3.82	4T	18.66	7.14	1T	HPF	<b>1.95</b>
bone_subx.n26c100	3 M	101 M	2.37	4.09	16T	78.74	4.65	32T	8.27	4.77	8T	17.29	9.36	1T	HPF	<b>2.14</b>
bone_subx.n6c10	3 M	23 M	0.52	1.28	16T	19.45	2.97	16T	0.83	1.45	4T	4.33	2.27	32T	HPF	<b>1.07</b>
bone_subx.n6c100	3 M	23 M	0.53	2.83	8T	19.62	3.29	16T	0.98	2.16	8T	4.35	2.90	24T	HPF	<b>1.28</b>
liver.n26c10	4 M	108 M	2.42	11.01	32T	86.56	9.33	32T	1.02	<b>3.81</b>	1T	13.12	9.17	1T	HPF	4.53
liver.n26c100	4 M	108 M	2.44	17.88	6T	85.71	10.48	32T	1.00	7.00	1T	17.11	15.67	1T	HPF	<b>5.72</b>
liver.n6c10	4 M	25 M	0.56	4.01	6T	21.21	6.06	16T	0.64	<b>3.79</b>	1T	4.35	5.51	1T	HPF	4.40
liver.n6c100	4 M	25 M	0.56	8.31	8T	22.14	6.73	16T	0.64	7.91	1T	4.41	11.11	1T	HPF	<b>5.70</b>
Surface fitting																
LB07-bunny-lrg	49 M	300 M	6.47	<b>2.10</b>	16T	260.38	37.73	32T	9.01	4.51	4T	51.78	3.64	8T	EIBFS	6.38

improvement as it rarely dips below its single threaded performance and often gives at least a 2x speed-up.

## 5 DISCUSSION

### 5.1 Serial Algorithms

It is clear from the results that the pseudo-flow-based algorithms have the best overall performance. Measured on solve time, EIBFS performed the best of the serial algorithms, which aligns with the results presented in [25]. However, if we look at the total time, the HPF algorithm performs the best on the majority of the datasets, which does not align with the results from [25]. We see two possible explanations for this:

- 1) [25] use the H-FIFO configuration for HPF, which according to our results, is consistently outperformed by H-LIFO. This significantly improves the HPF results in our comparison.

- 2) For the most of the datasets benchmarked in [25], they use 32-bit pointers, which significantly reduces the size of the Node and Arc data structures. This generally results in better performance (as demonstrated in our experiments).

Something we cannot explain, is why the total timings from our experiments are not significantly lower than those from [25], given the superior hardware used in our experiments. On the contrary, when using EIBFS, we actually take longer than them to build the graph and solve the problem, even for the `adhead.n6c100` dataset where they too use 64-bit pointers. Even though their EIBFS implementation has a slightly smaller memory footprint than EIBFS-I and avoids the overhead from index-based referencing, we do not see how this could account for the difference in observed performance. To investigate this further, we would have to also benchmark the exact EIBFS implementation used in [25]. However, as previously mentioned in Section 4.2, this implementation cannot

process some of the larger benchmark datasets. In the interest of consistency, we have used the same implementation for all tests.

For all algorithms, it is clear that the implementation details have a large effect on the performance and practicality of an algorithm. Optimizing for cache efficiency seems to be of particular importance since optimizations such as arc packing and smaller data structures have large effects on the solve times. However, the benefit of arc packing is smaller for the total times, as the extra initialization step incurs additional overhead. Furthermore, as seen Table 1 it also increases the memory usage meaning that users have to choose between increased performance or lower memory usage. This trade-off is important as the memory footprint of an algorithm directly dictates the maximum size of the problems that are practical to solve on a given system. As shown in Table 1, MBK, and the parallel implementations based on it, has the smallest memory footprint closely followed by EIBFS-I-NR. This allows MBK to handle datasets over twice the size of some of the other algorithms.

## 5.2 Parallel Algorithms

The superior performance of the Liu-Sun algorithm, compared to the other parallel algorithms aligns with previous results [49] and expectations [59, 60]. While the algorithm cannot match the serial algorithms on small to medium datasets, it is clear that it scales well on larger datasets, where our results show it being more than five times faster than the fastest serial algorithm.

As expected due to its node-based parallelism, P-PPR scales best with a large number of parallel threads. As shown in Table 3 and Fig. 8, it achieves its best results with 32 threads for nearly all datasets. For the block based algorithms, they typically achieve their best median speed-up with 4-8 threads. However, both Liu-Sun and P-ARD achieve their maximum speed-up with 32 threads which, as shown in Fig. 7, is because large datasets allow these algorithms to utilize more threads. We attribute the poor performance of Strandmark-Kahl to convergence issues when splitting the graph into many blocks [69].

For practical use, only the Liu-Sun and P-ARD implementations appear relevant as is. And of the two, Liu-Sun is clearly the superior one, especially when build time is taken into consideration. While the node-based parallelism of P-PPR seems like a good idea in theory, the synchronization overhead results in very poor overall performance. Thus, even with 32 threads, it often cannot match the performance of the serial algorithms. On the other hand, while block-based parallelism appears particularly well suited for large datasets, their scaling is much less predictable for small to medium datasets. This can make it non-trivial to select an optimal thread count, which makes them less practical.

Moreover, the performance of the block-based algorithms also depends on a reasonable way of splitting the datasets into blocks. Since the optimal blocking strategy depends on the specific graph, it is possible that our blocks were not optimal for all datasets which would influence our performance measurements.

Finally, the Liu-Sun implementation tested in our experiments relies on the MBK implementation, which, as we show, is not as fast as the HPF and EIBFS implementations. As adaptive bottom-up merging can in theory be used with any min-cut/max-flow algorithm, one might consider replacing BK with HPF or EIBFS for improved performance. However, it is important to remember that for the bottom-up merging to be fast, it requires an algorithm which is fast when changing the graph and recomputing the min-cut/max-flow solution. Although EIBFS allows this [25], our preliminary

tests showed that the overhead of changing the graph and updating the solution is significantly higher for EIBFS than BK, which means that parallel EIBFS based on bottom-up merging is often considerably slower than serial EIBFS, even for large datasets. To our knowledge, the HPF implementation tested in the paper does not support dynamically updating the min-cut/max-flow solution. However, if HPF or EIBFS can be implemented such that they can match the performance of BK for dynamic graph problems, using them in combination with a bottom-up merging approach could be worthwhile.

## 6 CONCLUSIONS

We performed an extensive comparison of the state-of-the-art generic serial and parallel min-cut/max-flow algorithms, some of which continue to see extensive use for optimization problems in the computer vision community.

### 6.1 Serial Algorithms

For the serial min-cut/max-flow algorithms, we have tested a total of eight different implementations across four of the fastest and most popular algorithms: PPR, BK, EIBFS, and HPF. These four algorithms include representatives for the three families of min-cut/max-flow algorithms: augmenting paths, push-relabel and pseudoflow.

Our results clearly show that the two pseudoflow algorithms, EIBFS and HPF, are significantly faster than the other algorithms, which leads us to conclude that these two algorithms should be the first choice for anyone looking for a fast serial min-cut/max-flow algorithm for static computer vision problems. For a comparison with dynamic problems, we refer to [25].

Based on our results, we recommend the HPF algorithm with the H-LIFO configuration, as it performs best for the majority of the problems when looking at the total time spent building the graph and finding the min-cut/max-flow solution. However, the EIBFS algorithm (EIBFS-I implementation) is a very close contender and can easily replace HPF with little impact on performance. The BK algorithm (MBK implementation) falls significantly behind the two pseudoflow algorithms, but still provides good performance for most of the problems tested in this paper. Meanwhile, the PPR algorithm represented by HI-PPR is much slower than the three other algorithms.

If memory usage is of chief concern, the MBK implementation of the BK algorithm and EIBFS-I-NR implementation of the EIBFS algorithm are both good options, as they use significantly less memory than the reference EIBFS implementations and HPF.

### 6.2 Parallel Algorithms

We tested four different parallel algorithms for min-cut/max-flow problems: parallel PPR (P-PPR), adaptive bottom-up merging (Liu-Sun), dual decomposition (Strandmark-Kahl), and region discharge (P-ARD). Of these, we found adaptive bottom-up merging, as proposed by Liu and Sun [49], to be the best parallel approach, as our implementation of it outperformed the other parallel algorithms overall. Although each algorithm has the fastest solve time for at least a few of the benchmark problems, Liu-Sun performed the best overall.

Compared to serial algorithms, Liu-Sun could only match the performance serial MBK for smaller problems, but was several times faster than the fastest serial algorithm on large problems. However,

for small to medium problems, a modern serial algorithm like EIBFS or HPF still provides superior performance. As a rule of thumb, we recommend considering parallel algorithms for problems over 5 M nodes or where a serial algorithm uses over 5 seconds.

Regarding scaling, P-ARD is not able to scale as well with the number of threads as Liu-Sun, while Strandmark-Kahl is only able to utilize up to eight threads. P-PPR on the other hand scales well with the number of threads, however, it still performs worse than Liu-Sun in most cases, even when using several times more parallel threads. Unfortunately, the optimal blocking strategy and an optimal number of threads appears to depend on the dataset. However, for Liu-Sun, the performance generally improves up to eight threads, but appears to scale way beyond that for very large problems.

## 7 PERSPECTIVES

We now provide perspectives regarding possible future developments of min-cut/max-flow methods — both for serial and parallel algorithms — as well as how these may fit into the future of computer vision.

### 7.1 Serial Algorithms

For serial algorithms, our results indicate that the pseudo-flow algorithms are the most promising area for new developments of efficient min-cut/max-flow algorithms in computer vision, as they consistently perform best. Furthermore, the theoretical framework is less restrictive than for AP for PPR algorithms, which gives lots of options for innovative new solution strategies.

Furthermore, we think there are significant performance improvements to be gained from further improving the algorithm implementations — especially with a focus on memory use and cache efficiency. In particular, methods to perform arc (and node) packing faster and with lower memory requirements could result in significant benefits since the extra initialization step incurs a lot of memory and run-time overhead.

### 7.2 Parallel Algorithms

For the parallel algorithms, combining adaptive bottom-up merging with pseudoflow algorithms is an attractive direction to improve performance. Another option would be to explore hybrid block-based parallel algorithms, which uses a pseudoflow algorithm for the initial min-cut/max-flow computations but switches to BK once the iterative stage starts. Additionally, the parallel implementations should take advantage of parallelism when building the graph, which is done serially.

Choosing an optimal blocking strategy for the block-based parallel algorithms is an open problem. Currently, blocks must be specified a priori based on user assumptions and knowledge of the underlying graph structure. Designing robust automated blocking strategies would therefore make these algorithms much more practical and could also increase performance in cases where a user may not be an expert in the specific graph construction used.

### 7.3 Min-cut/max-flow in Modern Computer Vision

It is no secret that the field of computer vision is currently dominated by deep learning. In that context, it is highly relevant to consider the future role of traditional computer vision tools, such as min-cut/max-flow algorithms.

For 3D images used in medical imaging and materials science research [50], it is common to have images where no relevant training data is available. Here, segmentation methods based on min-cut/max-flow continue to play an important role since they can work without training data and allow geometric prior knowledge to be incorporated. Furthermore, while modern 3D images can already be very large (many GB per image), dynamic imaging (3D+time) with high acquisition rates is now also possible [20, 54]. As a result, computational efficiency is paramount to be able to process this ever increasing amount of data and thus parallel min-cut/max-flow algorithms could prove particularly useful.

Finally, as mentioned in [53], there is an agreement that the performance of deep learning-based segmentation methods has started to plateau, and investigating how to integrate CNNs with ‘classical’ approaches should be pursued. Already, combinations with active contours have shown promising results [27, 56, 65] and a combination of CNNs and min-cut/max-flow methods could lead to new advances. However, as training deep learning involves repeated forward and backward passes through a model, it is crucial that the min-cut/max-flow algorithms are fast, efficient, and are able to leverage the parallelized/distributed nature of deep neural net training.

## REFERENCES

- [1] Gene M Amdahl. “Validity of the single processor approach to achieving large scale computing capabilities”. In: *Proceedings of the April 18-20, 1967, spring joint computer conference*. 1967, pp. 483–485.
- [2] Richard Anderson and Joao C. Setubal. “A parallel implementation of the push-relabel algorithm for the maximum flow problem”. In: *Journal of Parallel and Distributed Computing (JPDC)* 29.1 (1995), pp. 17–26.
- [3] Chetan Arora et al. “An efficient graph cut algorithm for computer vision problems”. In: *Proceedings of the European Conference on Computer Vision (ECCV)*. 2010, pp. 552–565.
- [4] David A Bader and Vipin Sachdeva. *A cache-aware parallel implementation of the push-relabel network flow algorithm and experimental evaluation of the gap relabeling heuristic*. Tech. rep. Georgia Institute of Technology, 2006.
- [5] J Andreas Bærentzen et al. *Guide to computational geometry processing: foundations, algorithms, and methods*. Springer Science & Business Media, 2012.
- [6] Niklas Baumstark, Guy Blelloch, and Julian Shun. “Efficient implementation of a synchronous parallel push-relabel algorithm”. In: *Proceedings of the European Symposium on Algorithms (ESA)*. 2015, pp. 106–117.
- [7] Endre Boros, Peter L Hammer, and Xiaorong Sun. *Network flows and minimization of quadratic pseudo-Boolean functions*. Tech. rep. Technical Report RRR 17-1991, RUTCOR, 1991.
- [8] Stephen Boyd and Lieven Vandenbergh. *Convex optimization*. Cambridge University Press, 2004.
- [9] Yuri Boykov and Vladimir Kolmogorov. “An Experimental Comparison of Min-Cut/Max-Flow Algorithms for Energy Minimization in Vision”. In: *IEEE Transactions on Pattern Analysis and Machine Intelligence (PAMI)* 26.9 (2004), pp. 1124–1137.

- [10] Yuri Boykov, Olga Veksler, and Ramin Zabih. “Markov random fields with efficient approximations”. In: *Proceedings of the IEEE Conference on Computer Vision and Pattern Recognition (CVPR)*. 1998, pp. 648–655.
- [11] Bala G Chandran and Dorit S Hochbaum. “A computational study of the pseudoflow and push-relabel algorithms for the maximum flow problem”. In: *Operations Research* 57.2 (2009), pp. 358–376.
- [12] Xinjian Chen and Lingjiao Pan. “A survey of graph cuts/graph search based medical image segmentation”. In: *IEEE Reviews in Biomedical Engineering (RBME)* 11 (2018), pp. 112–124.
- [13] Boris V Cherkassky and Andrew V Goldberg. “On implementing the push—relabel method for the maximum flow problem”. In: *Algorithmica* 19.4 (1997), pp. 390–410.
- [14] Thomas H Cormen et al. *Introduction to algorithms*. MIT press, 2009.
- [15] Andrew DeLong and Yuri Boykov. “A scalable graph-cut algorithm for ND grids”. In: *Proceedings of the IEEE Conference on Computer Vision and Pattern Recognition (CVPR)*. 2008, pp. 1–8.
- [16] Jan Egger et al. “Nugget-cut: a segmentation scheme for spherically-and elliptically-shaped 3D objects”. In: *Joint Pattern Recognition Symposium (JPRS)*. 2010, pp. 373–382.
- [17] B. Fishbain, Dorit S. Hochbaum, and Stefan Mueller. “A competitive study of the pseudoflow algorithm for the minimum s–t cut problem in vision applications”. In: *Journal of Real-Time Image Processing (JRTIP)* 11.3 (2016), pp. 589–609.
- [18] Lester Randolph Ford Jr and Delbert Ray Fulkerson. *Flows in networks*. Princeton university press, 1962.
- [19] Daniel Freedman and Petros Drineas. “Energy minimization via graph cuts: Settling what is possible”. In: *Proceedings of the IEEE Conference on Computer Vision and Pattern Recognition (CVPR)*. 2005, pp. 939–946.
- [20] Francisco García-Moreno et al. “Using X-ray tomography to explore the dynamics of foaming metal”. In: *Nature communications* 10.1 (2019), pp. 1–9.
- [21] Andrew V Goldberg. “Processor-efficient implementation of a maximum flow algorithm”. In: *Information Processing Letters* 38.4 (1991), pp. 179–185.
- [22] Andrew V Goldberg. “The partial augment–relabel algorithm for the maximum flow problem”. In: *Proceedings of the European Symposium on Algorithms (ESA)*. 2008, pp. 466–477.
- [23] Andrew V Goldberg. “Two-level push-relabel algorithm for the maximum flow problem”. In: *International Conference on Algorithmic Applications in Management*. 2009, pp. 212–225.
- [24] Andrew V Goldberg and Robert E Tarjan. “A new approach to the maximum-flow problem”. In: *Journal of the ACM (JACM)* 35.4 (1988), pp. 921–940.
- [25] Andrew V Goldberg et al. “Faster and More Dynamic Maximum Flow by Incremental Breadth-First Search”. In: *Proceedings of the European Symposium on Algorithms (ESA)*. 2015, pp. 619–630.
- [26] Andrew V Goldberg et al. “Maximum Flows by Incremental Breadth-First Search”. In: *Proceedings of the European Symposium on Algorithms (ESA)*. 2011, pp. 457–468.
- [27] Lihong Guo et al. “Learned snakes for 3D image segmentation”. In: *Signal Processing* 183 (2021), p. 108013.
- [28] Zhihui Guo et al. “Deep LOGISMOS: deep learning graph-based 3D segmentation of pancreatic tumors on CT scans”. In: *Proceedings of the IEEE International Symposium on Biomedical Imaging (ISBI)*. 2018, pp. 1230–1233.
- [29] Peter L Hammer, Pierre Hansen, and Bruno Simeone. “Roof duality, complementation and persistency in quadratic 0–1 optimization”. In: *Mathematical Programming* 28.2 (1984), pp. 121–155.
- [30] Dorit S. Hochbaum. “The pseudoflow algorithm: A new algorithm for the maximum-flow problem”. In: *Operations Research* 56.4 (2008), pp. 992–1009.
- [31] Dorit S. Hochbaum and James B. Orlin. “Simplifications and speedups of the pseudoflow algorithm”. In: *Networks* 61.1 (2013), pp. 40–57.
- [32] Bo Hong and Zhengyu He. “An asynchronous multithreaded algorithm for the maximum network flow problem with non-blocking global relabeling heuristic”. In: *IEEE Transactions on Parallel and Distributed Systems (TPDS)* 22.6 (2010), pp. 1025–1033.
- [33] Hossam Isack et al. “Efficient optimization for hierarchically-structured interacting segments (HINTS)”. In: *Proceedings of the IEEE Conference on Computer Vision and Pattern Recognition (CVPR)*. 2017, pp. 1445–1453.
- [34] Hiroshi Ishikawa. “Exact optimization for Markov random fields with convex priors”. In: *IEEE Transactions on Pattern Analysis and Machine Intelligence (PAMI)* 25.10 (2003), pp. 1333–1336.
- [35] Ondřej Jamriška and Daniel Šýkora. *GridCut. Version 1.3*. <https://gridcut.com>. Accessed 2020-06-12. 2015.
- [36] Ondřej Jamriška, Daniel Šýkora, and Alexander Hornung. “Cache-efficient Graph Cuts on Structured Grids”. In: *Proceedings of the IEEE Conference on Computer Vision and Pattern Recognition (CVPR)*. 2012, pp. 3673–3680.
- [37] Patrick M. Jensen, Anders B. Dahl, and Vedrana A. Dahl. “Multi-Object Graph-Based Segmentation With Non-Overlapping Surfaces”. In: *Proceedings of the IEEE Conference on Computer Vision and Pattern Recognition Workshops (CVPRW)*. 2020, pp. 976–977.
- [38] Patrick M. Jensen and Niels Jeppesen. *Max-Flow/Min-Cut Algorithms*. <https://doi.org/10.5281/zenodo.4912409>. Accessed 2021-06-08. DOI: 10.5281/zenodo.4912409.
- [39] Niels Jeppesen et al. “Sparse Layered Graphs for Multi-Object Segmentation”. In: *Proceedings of the IEEE Conference on Computer Vision and Pattern Recognition (CVPR)*. 2020, pp. 12777–12785.
- [40] S Kashyap, H Zhang, and M Sonka. “Accurate Fully Automated 4D Segmentation of Osteoarthritic Knee MRI”. In: *Osteoarthritis and Cartilage* 25 (2017), S227–S228.
- [41] Anna Khoreva et al. “Simple does it: Weakly supervised instance and semantic segmentation”. In: *Proceedings of the IEEE Conference on Computer Vision and Pattern Recognition (CVPR)*. 2017, pp. 876–885.
- [42] Pushmeet Kohli and Philip H.S. Torr. “Dynamic graph cuts for efficient inference in Markov random fields”. In: *IEEE Transactions on Pattern Analysis and Machine Intelligence (PAMI)* 29.12 (2007), pp. 2079–2088.
- [43] Vladimir Kolmogorov and Carsten Rother. “Minimizing non-submodular functions with graph cuts—a review”. In: *IEEE Transactions on Pattern Analysis and Machine Intelligence (PAMI)* 29.7 (2007), pp. 1274–1279.



- [44] Vladimir Kolmogorov and Ramin Zabih. "Computing visual correspondence with occlusions using graph cuts". In: *Proceedings of the International Conference on Computer Vision (ICCV)*. Vol. 2. 2001, pp. 508–515.
- [45] Vladimir Kolmogorov and Ramin Zabih. "What energy functions can be minimized via graph cuts?" In: *IEEE Transactions on Pattern Analysis and Machine Intelligence (PAMI)* 26.2 (2004), pp. 147–159.
- [46] Kyungmoo Lee et al. "Multiresolution LOGISMOS graph search for automated choroidal layer segmentation of 3D macular OCT scans". In: *Medical Imaging 2020: Image Processing*. Vol. 11313. International Society for Optics and Photonics. 2020, 113130B.
- [47] Victor Lempitsky and Yuri Boykov. "Global optimization for shape fitting". In: *Proceedings of the IEEE Conference on Computer Vision and Pattern Recognition (CVPR)*. 2007, pp. 1–8.
- [48] Kang Li et al. "Optimal surface segmentation in volumetric images—a graph-theoretic approach". In: *IEEE Transactions on Pattern Analysis and Machine Intelligence (PAMI)* 28.1 (2005), pp. 119–134.
- [49] Jiangyu Liu and Jian Sun. "Parallel Graph-cuts by Adaptive Bottom-up Merging". In: *Proceedings of the IEEE Conference on Computer Vision and Pattern Recognition (CVPR)*. 2010, pp. 2181–2188.
- [50] Eric Maire and Philip John Withers. "Quantitative X-ray tomography". In: *International materials reviews* 59.1 (2014), pp. 1–43.
- [51] Max-flow problem instances in vision. <https://vision.cs.uwaterloo.ca/data/maxflow>. Accessed 2021-02-05.
- [52] Min-Cut/Max-Flow Problem Instances for Benchmarking. <https://doi.org/10.5281/zenodo.4905882>. Accessed 2021-06-07. DOI: 10.5281/zenodo.4905882.
- [53] Shervin Minaee et al. "Image segmentation using deep learning: A survey". In: *IEEE Transactions on Pattern Analysis and Machine Intelligence (PAMI)* (2021).
- [54] Rajmund Mokso et al. "GigaFRoST: the gigabit fast read-out system for tomography". In: *Journal of synchrotron radiation* 24.6 (2017), pp. 1250–1259.
- [55] Bo Peng, Lei Zhang, and David Zhang. "A survey of graph theoretical approaches to image segmentation". In: *Pattern Recognition* 46.3 (2013), pp. 1020–1038.
- [56] Sida Peng et al. "Deep snake for real-time instance segmentation". In: *Proceedings of the IEEE Conference on Computer Vision and Pattern Recognition (CVPR)*. 2020, pp. 8533–8542.
- [57] Yi Peng et al. "JF-Cut: A parallel graph cut approach for large-scale image and video". In: *IEEE Transactions on Image Processing* 24.2 (2015), pp. 655–666.
- [58] Carsten Rother et al. "Optimizing binary MRFs via extended roof duality". In: *Proceedings of the IEEE Conference on Computer Vision and Pattern Recognition (CVPR)*. 2007, pp. 1–8.
- [59] Alexander Shekhovtsov and Václav Hlaváč. "A distributed mincut/maxflow algorithm combining path augmentation and push-relabel". In: *International Journal of Computer Vision (IJCV)* 104.3 (2013), pp. 315–342.
- [60] Petter Strandmark and Fredrik Kahl. "Parallel and Distributed Graph Cuts by Dual Decomposition". In: *Proceedings of the IEEE Conference on Computer Vision and Pattern Recognition (CVPR)*. 2010, pp. 2085–2092.
- [61] Nima Tajbakhsh et al. "Embracing imperfect datasets: A review of deep learning solutions for medical image segmentation". In: *Medical Image Analysis* 63 (2020), p. 101693.
- [62] Tanmay Verma and Dhruv Batra. "MaxFlow Revisited: An Empirical Comparison of Maxflow Algorithms for Dense Vision Problems". In: *Proceedings of the British Machine Vision Conference (BMVC)*. 2012, pp. 1–12.
- [63] Vibhav Vineet and P J Narayanan. "CUDA cuts: Fast graph cuts on the GPU". In: *Proceedings of the IEEE Conference on Computer Vision and Pattern Recognition Workshops (CVPRW)*. 2008, pp. 1–8.
- [64] Yao Wang and Reinhard Beichel. "Graph-based segmentation of lymph nodes in CT data". In: *Proceedings of the International Symposium on Visual Computing (ISVC)*. 2010, pp. 312–321.
- [65] Udaranga Wickramasinghe et al. "Voxel2mesh: 3d mesh model generation from volumetric data". In: *Proceedings of the International Conference on Medical Image Computing and Computer Assisted Intervention (MICCAI)*. Springer. 2020, pp. 299–308.
- [66] Xiaodong Wu and Danny Z Chen. "Optimal net surface problems with applications". In: *Proceedings of the International Colloquium on Automata, Languages, and Programming (ICALP)*. 2002, pp. 1029–1042.
- [67] Yin Yin et al. "LOGISMOS—layered optimal graph image segmentation of multiple objects and surfaces: cartilage segmentation in the knee joint". In: *IEEE Transactions on Medical Imaging (T-MI)* 29.12 (2010), pp. 2023–2037.
- [68] Miao Yu, Shuhan Shen, and Zhanyi Hu. "Dynamic Graph Cuts in Parallel". In: *IEEE Transactions on Image Processing* 26.8 (2017).
- [69] Miao Yu, Shuhan Shen, and Zhanyi Hu. "Dynamic Parallel and Distributed Graph Cuts". In: *IEEE Transactions on Image Processing* 25.12 (2015), pp. 5511–5525.